Optimum solar sail configurations based on astrodynamics, designer materials, sizing and geometries: an example of astro-elastic and astro-viscoelastic system engineering

(Received: Dec 26, 2019. Revised: June 6, 2020. Accepted: July 1, 2020)

Harry H. Hilton[1,2] and Steven J. D'Urso[1]

Abstract
A generalized analysis is formulated that extends wind sail aerodynamics to a designer system engineering of solar sails through equivalent astrodynamics, astro-elasticity, astro-viscoelasticity, morphing and optimization. The analytical formulation is cast in terms of an inverse calculus of variations problem that leads to solutions yielding optimum solar sail material properties, sizing and geometries subject to preselected constraints, such as maximum thrust, high strength, minimum weight, stability and control, etc. A relatively simple less inclusive illustrative example is also presented.

1. Introduction

To coin a phrase, astro-elasticity and astro-viscoelasticity are the space parallels to atmospheric aeroelasticity [1 – 19] and aero-viscoelasticity [20 – 41] except that aerodynamic lift and drag forces are replaced by similar solar wind forces. In the final analysis, it is the "wind" generated velocity squared - whether atmospheric or solar - that produces the lift and drag surface forces. Consequently with the exception of gravity forces, a flexible space vehicle sail exposed to solar winds behaves no differently than one exposed to atmospheric conditions, including temperature exposures.

It is to be noted that sails require no additional weight beside their own to deliver thrust, albeit a relatively small one compared to say chemically generated forces. However, solar sails may find use as augmentation thrust sources in unmanned long term voyages. Additionally, when not in use they may easily be retracted and stored.

The high demands for and the limited productivity by photo cells of electric power create a stark contrast in the operational needs of satellites and planetary probes. It, therefore, becomes imperative to devise alternate control and/or propulsion means for such vehicles. Similarly, space antenna dishes need to maintain their shapes in micro-gravity environments which can be realized through another optimum morphing protocol.

One such approach is the use of solar sails – a multidisciplinary set of problems combining materials, space structure morphing, magneto-electro-dynamics, stability and control, thrust, etc. Similarities and differences between aerodynamic [44] and solar sails need to be explored. However, in order to efficiently deploy both devices one must be able to morph them [45 – 51] into distinct optimal shapes. This can be be accomplished through the theoretical analyses and attendant protocols developed in [52] and further generalized in [53]. Also see the extensive bibliography in the latter publication.

The developed synthesis/designer approach has numerous advantages:

1. – optimum astrofoil shapes that yield high thrust, i.e. high lift, solar sails

[1] Aerospace Engineering Department, the Granger College of Engineering and [2]Computational and Data Sciences Division, National Center for Supercomputing Applications, University of Illinois at Urbana-Champaign, 104 South Wright Street, Urbana, IL 61801 USA

doi:10.3293/asdj.2020.54

2. – morphing of camber lines to produced specified motion, attitude control, $(L/D)_{max}$, etc.

3. – efficient weight control leading to highly flexible structures, and other prescribed tasks

4. – high strength to low weight ratio structures

5. – solar sails, space antenna dishes, etc. that can be readily morphed into desired shapes to satisfy prescribed tasks

The analysis and solution protocol developed in [52] is an inverse calculus of variation formulation subject to as as many restraints as desired to produce optimum material properties, geometries, stresses, deformations, etc. When applied to solar sail configurations, the protocol can select among other criteria, such as the following ratios $\frac{\text{high thrust}}{\text{low weight}}$, $\frac{\text{high thrust}}{\text{small area}}$, $\frac{\text{high maneuverability}}{\text{small energy expenditure}}$, etc.

When the vehicle is in a planet's shadow, the solar sail will experience low temperatures and behave elastically. On the opposite planetary side in full exposure of the Sun's rays the sail may then respond viscoelastically depending on its material composition.

In the final analysis, one must consider any sail producing lift and drag to behave like an ordinary flight vehicle wing, albeit with lesser rigidity than a typical flight vehicle one. More often than not, a sail is a thin limiting case warped plate represented by a camber line generated from an actual airfoil contour. As such, the astro-sail (astro-wing, solar sail) can be considered a double curvature plate with optimized variable thickness and functionally graded material properties. The sail's purpose is to produce lift that translates into propulsive thrust without generating an overabundance of drag forces.

Then the problem at hand is to synthesize an astro-sail wing driven by solar winds. This optimizing process includes the sail's shape, with an optimum astrofoil camber and shape to provide the prescribed thrust in conjunction with optimum material properties to provide sufficient rigidity and mass to withstand static and dynamic conditions, such as torsional divergence, control reversal, flutter, buffeting, etc., in a space environment as well as stability and control of the space vehicle including structural integrity and demanded performance of the solar sail and vehicle.

2. ANALYSIS

2.1 Governing relations

2.1.1 Elastic media

Consider a Cartesian coordinate system $x = \{x_i\} = \{x_1, x_2, x_3\}$ with the Einstein tensor notation in force. The elastic anisotropic constitutive relations then are

$$\sigma^e_{ij}(x,t) \;=\; E^0_{ijkl}\,[\epsilon^e_{kl}(x,t) \;-\; \alpha\,\vartheta(x,t)] \tag{1}$$

$$\epsilon^e_{ij}(x,t) \;=\; C^0_{ijkl}\,[\sigma^e_{kl}(x,t) \;+\; \alpha\,\vartheta(x,t)] \tag{2}$$

where T is the temperature of the solar sail, T_0 is the reference temperature at which the thermal expansions are zero, i.e. $\alpha\,\vartheta(T)\Big|_{T=T_0} = 0$, and

$$\vartheta(x,t) \;=\; T(x,t) \;-\; T_0 \tag{3}$$

For isothermal conditions $\vartheta = 0$. The temperature, of course, plays a major role in the position of a satellite during the sunlight, shadow and transitions of their orbits.

2.1.2 Viscoelastic media

When the sail is exposed to sunlight the temperatures of the material will rise. Since the sail will be made of composite materials one can expect viscoelastic rather than elastic behavior.

In the viscoelastic case, the constitutive relations are

$$\sigma_{ij}(x,t) \;=\; \underbrace{\int_{-\infty}^{t} E_{ijkl}\left[x,t,t,T(x,t')\right]\,\frac{\partial\epsilon_{kl}(x,t')}{\partial t'}\,dt'}_{\text{mechanical strain contributions}} \;-\; \underbrace{\int_{-\infty}^{t} E^{T}_{ij}\left[x,t,t,T(x,t')\right]\,\frac{\partial\left[\alpha\,\vartheta(x,t')\right]}{\partial t'}\,dt'}_{\text{thermal expansion contributions}} \tag{4}$$

$$\epsilon_{ij}(x,t) \;=\; \int_{-\infty}^{t} C_{ijkl}\left[x,t,t,T(x,t')\right]\,\frac{\partial\sigma_{kl}(x,t')}{\partial t'}\,dt' \;+\; \int_{-\infty}^{t} C^{T}_{ij}\left[x,t,t,T(x,t')\right]\,\frac{\partial\left[\alpha\,\vartheta(x,t)\right]}{\partial t'}\,dt' \tag{5}$$

In the advent of constant or time independent temperatures, these relations reduce to

$$\sigma_{ij}(x,t) \;=\; \int_{-\infty}^{t} E_{ijkl}\left[x,t-t,T(x)\right]\,\frac{\partial\epsilon_{kl}(x,t')}{\partial t'}\,dt' \tag{6}$$

$$\epsilon_{ij}(x,t) \;=\; \int_{-\infty}^{t} C_{ijkl}\left[x,t-t,T(x)\right]\,\frac{\partial\sigma_{kl}(x,t')}{\partial t'}\,dt' \tag{7}$$

The various moduli and compliances can be generically represented by separate Prony series [42], such that at constant temperatures

$$E(t) \;=\; E_{\infty} \;+\; \sum_{n=1}^{N} E_n \exp\left(-\frac{t}{\tau_n}\right) \quad \text{with} \quad E_0 \;=\; E_{\infty} \;+\; \sum_{n=1}^{N} E_n \tag{8}$$

Substituting into (6) and integrating by parts, yields

$$\sigma_{ij}(x,t) \;=\; E_{ijkl0}\,\epsilon_{kl}(x,t) \;-\; \int_{0}^{t} \underbrace{\sum_{n=1}^{N}\sum_{\substack{k=1\\ l=1}}^{3} \frac{E_{\underline{ijkl}n}}{\tau_{\underline{ijkl}n}} \exp\left(-\frac{t-t'}{\tau_{\underline{ijkl}n}}\right)}_{=\;\phi(t-t')}\,\epsilon_{kl}(x,t')\;dt' \tag{9}$$

where $\phi_{ijkl}(t)$ are the anisotropic relaxation functions. A similar construction can be carried out for Eq. (7) with $\psi_{ijkl}(t)$ the anisotropic creep functions. Both of these later two functions as well as moduli and compliances can additionally be nonhomogeneous such as $E_{ijkl}(x,t)$, etc.

2.1.3 Viscoplastic media

The fundamental difference between viscoelasticity and viscoplasticity is that the second medium exhibits one or more yield points and distinct constitutive relations in each region. This may occur during cold flights but generally will not take place under elevated or high temperatures. Since solar sails need to be folded and stored when not in use one may expect that they could be made of aluminum foil, cloth, polymer or composite materials. Consequently, one may expect them to behave regionally elastically or viscoelastically.

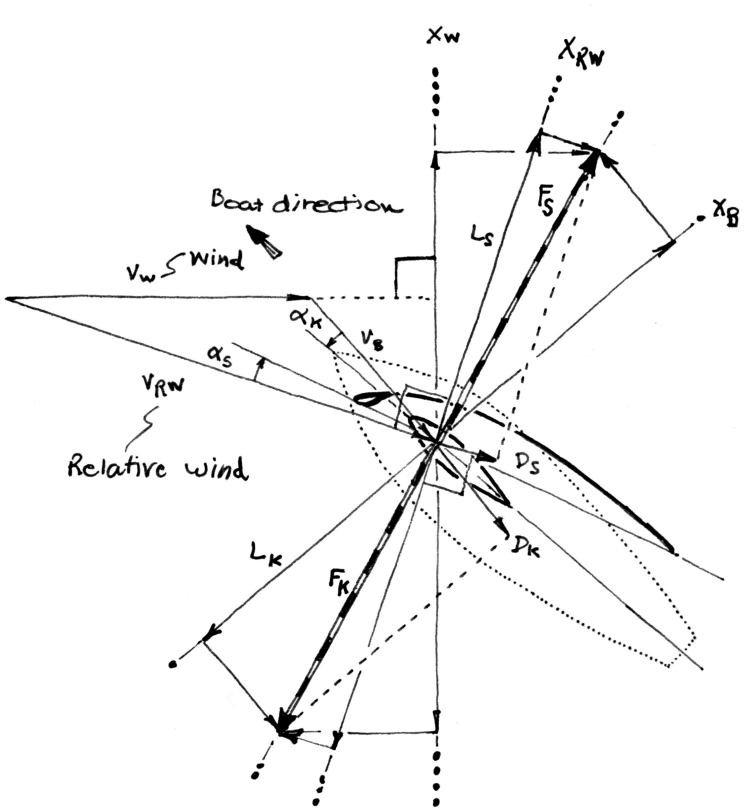

Figure 1: Typical force and motion vectors for sail and vehicle [68]

2.1.4 Astro-elastic/-viscoelastic issues

Basically the medium through which the solar sail and vehicle fly defines the problem at hand with major differences between aero-elasticity/viscoelasticity and astro-elasticity/viscoelasticity. The usual problems of torsional divergence, control reversal, flutter, buffeting, etc., fundamentally remain similar, except that atmospheric air is replaced by solar winds. The relatively low solar wind density may drive the vehicle velocity into supersonic or hypersonic regimes. In both media astro-elastic and astro-viscoelastic instabilities are driven by flight velocities regardless of their origin.

2.1.5 Solar wind astrodynamics and morphing of solar sails

Morphing to control tension at corners and thereby dictate sail shape can be readily accomplished through piezoelectric actuators with relatively limited power expenditures and can be employed for attitude and general flight control. A partial list of pertinent references are for aerodynamics [59 – 71] and for morphing [44 – 51].

2.1.6 Motion and control relations

Fig. 1 depicts the various force vectors arising from atmospheric lift and drag [68] that are directly transferable to solar sails by simply replacing atmospheric flows with solar winds.

2.2 Solar wind forces on sail

The equivalent driver to air velocity is the solar wind which is a plasma stream of charged particles that produces pressures at 1 AU in the range of 1 to 6 nPa

(1 to 6E-9 N/m^2). The dynamic pressure[1] p_{dyn} in nPa is a function of solar wind velocity V_{sw} in km/s and equals [54]

$$p_{dyn} \;=\; 1.6726 \otimes 10^{-6}\, \rho_{sw}\, V_{sw}^2 \;=\; 3.3452 \otimes 10^{-6}\, q_{sw} \tag{10}$$

where the solar wind density ρ_{sw} is 7 protons/cm^3. The solar wind speed varies approximately from 300 to 900 km/s with an average of 400 km/s. [55 – 57], which yields $1.0537 \le p_{dyn} \le 9.4836$ nPa.

The lift can then be obtained from

$$L(t) \;=\; \oint_A p_{dyn}(x,t)\, \vec{n}(x,t) \cdot \vec{k}(t)\, dA \tag{11}$$

where the unit vector $\vec{k}$ is normal to $\vec{V}_{sw}$ and $\vec{n}$ is the unit vector $\perp$ to the airfoil section surface and pointing into the sail section. This relation can also be written in a more conventional form as

$$L(t) \;=\; q_{sw} \int_A \underbrace{\frac{dc_l(x_2,t)}{d\alpha}\, \alpha(x_2,t)}_{\substack{= c_l(x_2),\ \text{the} \\ \text{section lift coefficient}}}\, dA \tag{12}$$

Similarly the drag of the sail can be expressed as

$$D(t) \;=\; \oint_A p_{dyn}(x,t)\, \vec{n}(x,t) \cdot \vec{i}(t)\, dA \;=\; q_{sw} \int_A \underbrace{\frac{dc_d(x_2,t)}{d\alpha}\, \alpha(x_2,t)}_{\substack{= c_d(x_2,t),\ \text{the} \\ \text{section drag coefficient}}}\, dA \tag{13}$$

with $\vec{i}$ the vector parallel to the flight velocity $\vec{V}_{sw}$. The following short hand definitions are introduced for the aero/astro-derivatives and for any stability derivatives as well

$$c_{l,\alpha}(x_2,t) \;\equiv\; \frac{dc_l(x_2,t)}{d\alpha} \quad \text{and} \quad c_{d,\alpha}(x_2,t) \;\equiv\; \frac{dc_d(x_2,t)}{d\alpha} \tag{14}$$

The pressure p_{dyn} depends on the shape of the solar sail, which in turn depends on how the sail is presented to the solar wind and what equilibrium shape it ultimately assumes subject to imposed constraints. This a classical closed loop astro-elastic or astro-viscoelastic problem where the solution feeds back through the input (solar wind pressure or lift and drag) to define the optimum shape and camber of the sail. The identical problem exists under atmospheric wind conditions for sails and flexible windmill blades.

For a 3–D Cartesian coordinate system $x = \{x_1, x_2, x_3\}$ Roman letters are used as subscripts. On the other hand, the 2–D coordinates $s_\gamma(x_1, x_2, t), \gamma = 1, 2$ are coordinates tangent to the sail surfaces in the $x_\gamma - x_3$ coordinate planes.

A thin flexible sail is basically a 2 – D membrane catenary that can sustain only tensions $\mathcal{T}_\gamma(x_1, x_2, t)$ with no bending and/or shear capabilities. The solar sail is attached to the vehicle by 3 or 4 tether lines depending on whether the sail is triangular or four sided. These are designated by $F_i^{(\mu)}(t)$, where the superscript μ refers to the particular line force and the subscript i refers to the Cartesian coordinate direction.

The radii of curvature of the middle surface are

$$\frac{1}{R_\gamma^{ms}(x,t)} \;=\; \underbrace{\frac{\partial^2 u_3(x,t)}{\partial x_{\underline{\gamma}}^2} \left[1 + \left(\frac{\partial u_3(x,t)}{\partial x_{\underline{\gamma}}}\right)^2\right]^{(-1/2)}}_{\text{nonlinear form}} \;\approx\; \underbrace{\frac{\partial^2 u_3(x,t)}{\partial x_{\underline{\gamma}}^2}}_{\substack{\text{linearized for} \\ \left(\frac{\partial u_3(x,t)}{\partial x_{\underline{\gamma}}}\right)^2 \ll 1}} \tag{15}$$

[1] nPa = nano Pascals

$$\text{with} \quad \gamma = 1, 2$$

where $u_3(x,t) \equiv u_3(x_1, x_2, t)$ is the deflection in the x_3-direction of the sail middle surface. For essentially very thin sails where the thickness $h \ll R_\gamma^{ms}$, one can assume that the middle surface normal strains are the only ones present in the system. For larger h's the resulting additional sail curvatures are prescribed to be caused by plane cross sections remaining plane, although the resulting strains become nonlinear functions of the radii of curvature [90]. The linear form of expression (15) is generally not realizable for flexible sails.

The shape of the sail described by u_3 may be specified as a given astrofoil either by specification or through morphing based on pre-selected constraints such as for instance $(L/D)_{max}$.

The angles $\varphi(x_1, x_2, t)$ between the tangents to the sail surface and the x_γ-axes are defined by

$$\varphi_\gamma \;=\; \arctan\left(\frac{\partial u_3}{\partial x_\gamma}\right) \tag{16}$$

The in-plane tensions $\mathcal{T}(x_1, x_2, t)$ are tangent to the surface and essentially can be considered as follower loads $\mathcal{T}_\gamma$ in the s_γ-directions with

$$\mathcal{T}_\gamma(x_1, x_2, t) \;=\; \mathcal{T}\cos\left[\varphi_\gamma(x_1, x_2, t)\right] \tag{17}$$

Similarly, the solar wind pressures $p_{dyn}(x_1, x_2, t)$, which are normal to the sail surface (Fig. 2), have components

$$p_\gamma(x_1, x_2, t) \;=\; \frac{p_{dyn}}{\tan\varphi_\gamma} \tag{18}$$

Therefore, the equilibrium conditions are

$$\text{geometry} \quad \Longrightarrow \quad ds_\gamma(x_1, x_2, t) \;=\; \sqrt{(dx_\gamma)^2 + (dx_3)^2} \quad \gamma = 1, 2 \tag{19}$$

$$\text{tensile strain tangent to sail surface} \quad \Longrightarrow \quad \epsilon_{\underline{\gamma\gamma}}(x,t) \;=\; \frac{ds_{\underline{\gamma}} - ds_{0_{\underline{\gamma}}}}{ds_{0_{\underline{\gamma}}}} \tag{20}$$

In an isotropic isothermal homogeneous medium the constitutive relations, the strains on the median surface designed by $\epsilon_{\underline{\gamma\gamma}}^{ms}$ are

$$\epsilon_{11}^{ms}(x,t) \;=$$

$$\begin{cases} C_{1111}^0\,\mathcal{T}_1(x,t) + C_{1122}^0\,\mathcal{T}_2(x,t) & \text{elastic} \\ \displaystyle\int_{-\infty}^{t} \left[C_{1111}(t-t')\frac{\partial\left[\mathcal{T}_1(x,t')\right]}{\partial t'} + C_{1122}(t-t')\frac{\partial\left[\mathcal{T}_2(x,t')\right]}{\partial t'}\right] dt' & \text{viscoelastic} \end{cases} \tag{21}$$

and

$$\epsilon_{22}^{ms}(x,t) \;=$$

$$\begin{cases} C_{1122}^0\,\mathcal{T}_1(x,t) + C_{1111}^0\,\mathcal{T}_2(x,t) & \text{elastic} \\ \displaystyle\int_{-\infty}^{t} \left[C_{1122}(t-t')\frac{\partial\left[\mathcal{T}_1(x,t')\right]}{\partial t'} + C_{1111}(t-t')\frac{\partial\left[\mathcal{T}_2(x,t')\right]}{\partial t'}\right] dt' & \text{viscoelastic} \end{cases} \tag{22}$$

For quasi steady-state sail conditions, negligible inertia,[2] and gravity, the forces on the sail are the wind pressure p_{dyn} and the in-plane tensions $\mathcal{T}$. These

[2] i.e. time independent wind velocity, no force build up in time, no sail flapping or flutter, etc.

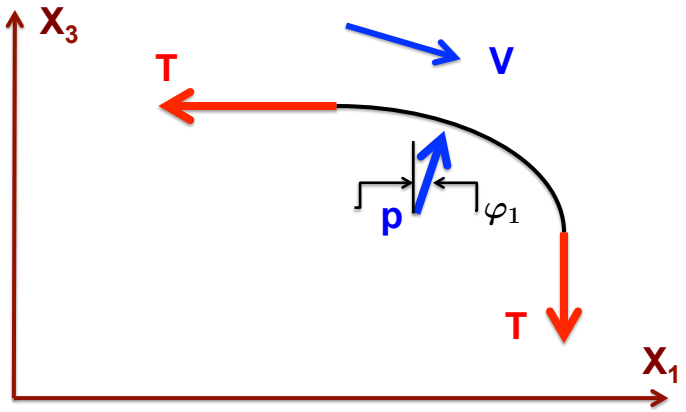

Figure 2: 3–D solar sail forces with $x_1 - x_3$ axes

conditions produce the following geometric and equilibrium relations (Fig. 2)

$$x_\gamma - \text{direction force equilibrium} \implies \sum F_\gamma = 0 \implies$$

$$\mathcal{L}_\gamma \left[p_{dyn}(x,t), \mathcal{T}(x,t), \varphi_\gamma(x,t)\right] = p_1(x,t) - \mathcal{T}_\gamma(x,t) = 0 \quad \text{with} \quad \gamma = 1,2 \tag{23}$$

with

$$\text{geometry} \implies \mathcal{L}_{\underline{\gamma}+2}\left[w(x,t), \varphi_{\underline{\gamma}}(x,t)\right] = \frac{\partial u_3(x,t)}{\partial x_\gamma} - \tan\left[\varphi_\gamma(x,t)\right] = 0$$

$$\text{with} \quad \gamma = 1,2 \tag{24}$$

Introducing a stress function $\psi(x,t)$ defined as [90]

$$\mathcal{T}_1 = h\frac{\partial^2 \psi}{\partial x_2^2} \quad \text{and} \quad \mathcal{T}_2 = h\frac{\partial^2 \psi}{\partial x_1^2} \tag{25}$$

where h is the sail thickness, leads to

$$\mathcal{L}_5 = \frac{\partial^4 \psi}{\partial x_1^4} + \frac{\partial^4 \psi}{\partial x_2^4} + \int_{-\infty}^{t} E(t-t')\frac{\partial^3 u_3(x,t')}{\partial x_1^2\, \partial t'}\frac{\partial^3 u_3(x,t')}{\partial x_2^2\, \partial t'}\, dt' = 0 \tag{26}$$

and

$$\mathcal{L}_6 = \mathcal{T}_3(x,t) + h\frac{\partial^2 \psi}{\partial x_2^2}\frac{\partial^2 u_3}{\partial x_1^2} + \frac{\partial^2 \psi}{\partial x_1^2}\frac{\partial^2 u_3}{\partial x_2^2} = 0 \tag{27}$$

The six unknowns are $u_3, \varphi_\gamma, \psi$ and $\mathcal{T}_\gamma$ and are defined by Eqs. (23), (24), (26) and (27). The solution protocol is outlined in Section 2.4.

These coupled governing relations are nonlinear and present scant hope of being decoupled or allowing a system analytic solution.

If morphing is applied or if the sail is permitted to assume an astrodynamical optimum camber, then the above aero/astro-derivatives – $c_{l,\alpha}$ and $c_{d,\alpha}$ – and possibly others, become parameters to be optimized subject to constraints such as maximum L/D ratios, minimum weight, maximum failure stress, etc.

The entire system of $\mathcal{L}_j$ equations is subject to M_c number of imposed preselected constraints $\mathcal{C}_m$ stated by

$$\mathcal{C}_m\left[\max\sigma, \max u_3, \omega, \text{weight}, \text{cost}, L/D_{max}, \cdots\right] = 0 \quad m = 1,2,3.\cdots, M_c \tag{28}$$

These constraints together with the aforementioned $\mathcal{L}_i$ relations form the system determining the optimized parameters necessary to meet the desired design conditions . See Section 2.4 and Fig. 6.

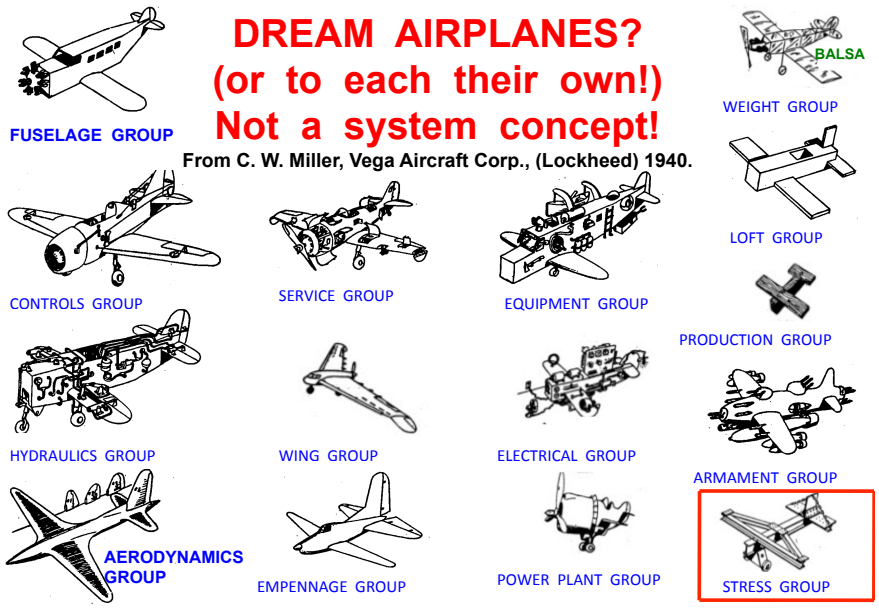

Figure 3: The worst case scenarios: isolations from and denials of pervasive system of systems concepts [58]

2.3 System engineering developments

A system engineering (holistic) approach to the synthesis (design) and optimization of entire or major vehicle portions is needed to confront these complex system engineering problems.

All major system component characteristics need to be considered in the context of interdependency and their interaction with whole vehicle. Advanced engineering methodologies are required to adequately characterize the various components and interfaces of the systems in a multi-disciplined evaluation in a holistic analysis.

Modeling of many of the system components has led to significant developments in the disciplines of tailored aerodynamics, aeroelasticity, stability, control, geometry, materials, structures, propulsion, performance, sizing, weight and cost, to mention a few. Unfortunately, except perhaps for aeroelasticity and control problems, they have been considered much too often in isolation from each other as single system elements rather than as part of an integrated closed loop system of systems. See the cartoon in Fig. 3 as extreme examples of possible exaggerated self importance and compartmentalization.

Economic feasibility of the systems is driven by the cost of fabrication, maintenance and operations. Multi-disciplined optimization allows for total system optimization but requires a balance of method fidelity to achieve the appropriately significant results.

Figs. 4 and 5 depict typical flow charts of a system engineering process showing the various details contributing to system protocols [87].

2.4 Designer system of system analysis – A generalized system engineering case

In [52] through an analytical formulation of inverse problems it was proven that elastic and viscoelastic material properties and structural sizing can be designed/tailored to render desired performances according to prior specifications and constraints. For instance, these protocols can be used to analytically design/engineer optimum elastic and/or relaxation moduli that guarantee say a

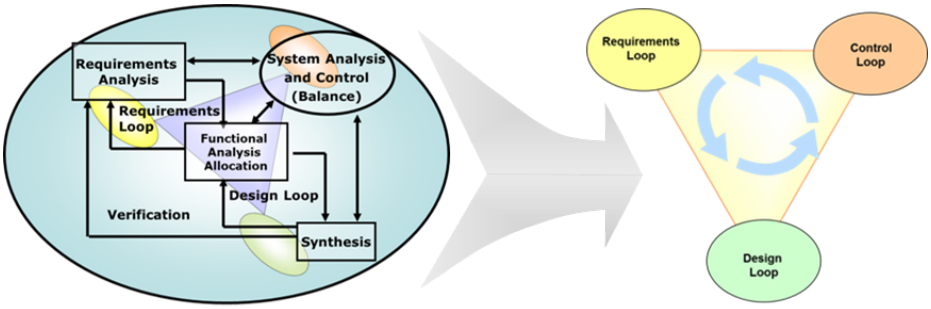

Figure 4: System engineering flow chart

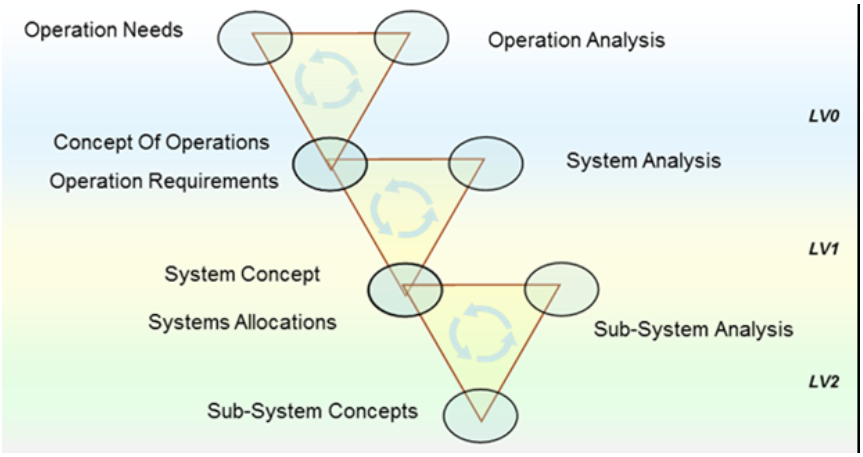

Figure 5: Schematic of system engineering process

maximum strength to weight ratio, maximum dissipation in a given time range or a maximum flutter speed or other constraints.

These formulations will now be generalized to designer systems of systems in a Cartesian space with co-ordinates $x = \{x_i\}$ with $i = 1, 2, 3$. The Einstein summation convention applies throughout. The number of systems is $\mathcal{P}$ and each system is identified by the superscript p. The state variables in each system are u_m^p and the ensemble of all state variables is designated by $\boldsymbol{u}$ as

$$\boldsymbol{u} = \boldsymbol{u}(x,t) = \{u_m^p(x,t)\} \qquad m = 1, 2, \cdots, \mathcal{M}^p \qquad \text{and} \qquad p = 1, 2, \cdots, \mathcal{P} \tag{29}$$

and each system has $\mathcal{M}^p$ number of variables.

The design parameters to be optimized are defined by

$$\boldsymbol{S} = \{S_n\} \qquad n = 1, 2, \cdots, \mathcal{N} \qquad \text{and} \qquad p = 1, 2, \cdots, \mathcal{P} \tag{30}$$

Some of the variables u_m and parameters S_m will appear in more than one system since each system and the system of systems are coupled.

Each of the systems has $\mathcal{Q}$ number of governing relations

$$\mathcal{L}_q^p(x, t, \boldsymbol{u}, \boldsymbol{S}) = 0 \qquad p = 1, 2, \cdots, \mathcal{P} \quad \text{and} \quad q = 1, 2, \cdots, \mathcal{Q}^p \tag{31}$$

with constraints

$$\mathcal{C}_\ell^p(x, t, \boldsymbol{u}, \boldsymbol{S}) = 0 \quad \ell = 1, 2, \cdots, \widehat{L} \qquad \text{and} \qquad p = 1, 2, \cdots, \mathcal{P} \tag{32}$$

This set of relations can now be individualized to each of the groups (i.e. system) of Fig. 3. Their total ensemble then forms the system of systems relations, which can be expressed as

$$\mathcal{L}(x, t, \boldsymbol{u}, \boldsymbol{S}) = \left\{\mathcal{L}_q^p(x, t, \boldsymbol{u}, \boldsymbol{S})\right\} = 0 \tag{33}$$

and

$$\mathcal{C}(x, t, \boldsymbol{u}, \boldsymbol{S}) = \{\mathcal{C}_\ell^p(x, t, \boldsymbol{u}, \boldsymbol{S})\} = 0 \tag{34}$$

Eqs. (33) and (34) are the governing relations for the optimized system of system and their solution for the parameter set $\boldsymbol{S}$ analytically defines its many details.

A brief outline of the protocol to be followed is shown in Fig. 6. This inverse procedure consists of the following:

1. Derive governing relations for the problem, which in generic form are shown in (31).

2. For each system formulate desired constraints $\mathcal{C}_\ell^p$ based on the prescribed specifications for the entire vehicle. However, in many cases these specifications may be derived requirements from the overall vehicle specifications in the system engineering sense.

3. Eliminate the spatial dependence of the state variables by applying Galerkin's procedure.

4. Solve the governing relations (31) for the remaining temporal functions

$$\widehat{\boldsymbol{u}}(\boldsymbol{S},t) = \int_a^b \boldsymbol{u}(x,t)\ \boldsymbol{u}_m^p(x,t)\ dx \qquad p = 1,2,\cdots,\mathcal{P} \ \text{ and } \ q = 1,2,\cdots,\mathcal{Q} \tag{35}$$

5. Eliminate the temporal dependence by least square fits or through the collocation method or by evaluation at prescribed life times

$$\widetilde{\boldsymbol{u}}(\boldsymbol{S}) = \widehat{\boldsymbol{u}}(\boldsymbol{S},t_{LF}) \tag{36}$$

or other specified times. Alternately, another specification could involve a time averaging process, such that

$$\widetilde{\boldsymbol{u}}(\boldsymbol{S}) \ = \ \frac{1}{t_{LF}} \int_0^{t_{LF}} \widehat{\boldsymbol{u}}(t')\ dt' \tag{37}$$

6. Formulate $\mathcal{M}\times\mathcal{P}$ simultaneous equations of the $\mathcal{M}\times\mathcal{P}$ unknown parameters through the application of Lagrangian multipliers λ_ℓ [72 – 73], such that

$$\frac{\partial}{\partial S_m^p}\left\{\widetilde{\boldsymbol{u}}(\boldsymbol{S}) \ + \ \lambda_\ell\, C_n^p(\boldsymbol{S})\right\} \ = 0 \quad m = 1,2,\cdots,\mathcal{M} \ \text{ and } p = 1,2,\cdots,\mathcal{P} \tag{38}$$

or any other proper expression(s) that one wishes to optimize.

7. After the Lagrangian multipliers λ_ℓ [72], [73], are eliminated in (38), one can solve the simultaneous algebraic transcendental equations for each and all S_m^p, thus realizing the optimized system of systems configuration.

8. Fig. 6 graphically summarizes and illustrates the above protocol.

3. An illustrative example

For the sake of simplicity consider a solar sail of fixed rectangular dimensions with constraints on optimum $\left(\frac{L}{D}\right)_{max}$ and $\left(\frac{\sigma_{fail}}{M_{sail}}\right)_{max}$. The symbol M_{sail} stands for the mass of the solar sail which is presumed to be a fiber/matrix composite, i.e. a nonhomogeneous anisotropic elastic or viscoelastic linear material. The question to be answered then is what are the mechanical properties of the

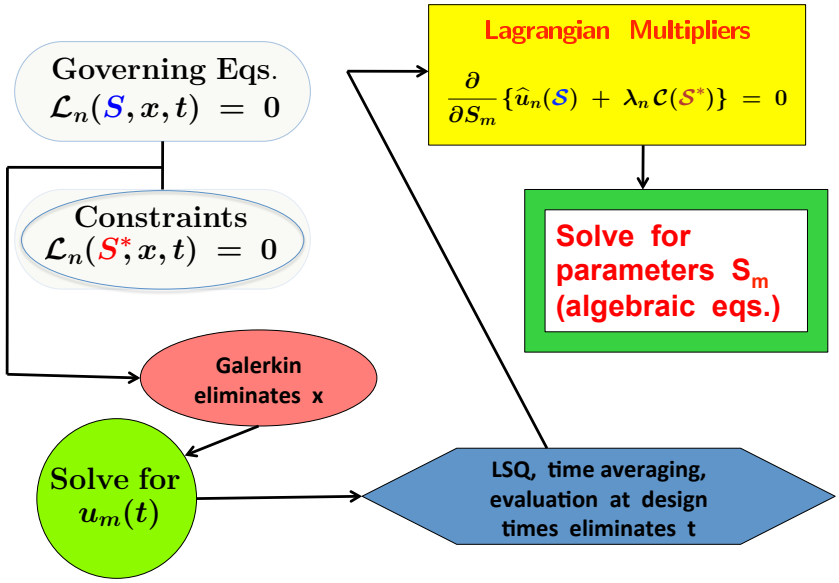

Figure 6: Designer calculus of variations flow chart [52]

sail to meet the imposed constraints. The sail x_1 and x_2 dimensions are a and b and the material is a single ply viscoelastic woven cloth. The temperature is considered as a constant throughout the sail – an assumption justified by the sail's thinness. Such a condition un-complicates the problem considerably, but far from totally, by removing transient loading conditions and the temperature dependent multiplicity of the relaxation moduli – see Figs. 8 and 9.

The Liebeck high lift L–1003 airfoil as characterized by its camber line – see Fig. 10 – was chosen to represent the solar sail [107 – 108]. In a real and more sophisticated synthesis process the actual camber shape could be system engineered along with other optimized parameters. The aerodynamic designer protocols and theory are presented in [59 – 71].

In the absence of any camber line data, the aerodynamic properties of the camber shaped sail were taken as those of the corresponding airfoil.

Cost has not been included in the present study, but Refs. [110 – 113] formulate and evaluate a number of pertinent cost functions.

4. Discussion

The simple illustrative example of Section 3. with its reduced number of optimized parameters and simplified sail loading compared to the general forces of Fig. 1 is, nevertheless instructive. The influence of temperature on viscoelastic materials as seen in Fig. 9, although not considered in this simple example, profoundly changes the material response time by orders of magnitude. The rather sparse available experimental data on viscoelastic multi-axial failures is exemplified by the typical 1-D display in Fig. 11 [95 – 102]. Fig. 12 illustrates the influence of various loading time conditions on ultimate failure times. Under constant flight velocities the space vehicle operates under relaxation protocols.

Figs. 13 and 14 present a few results. The first illustrates the importance of optimizing the variation of material property parameters in two directions by

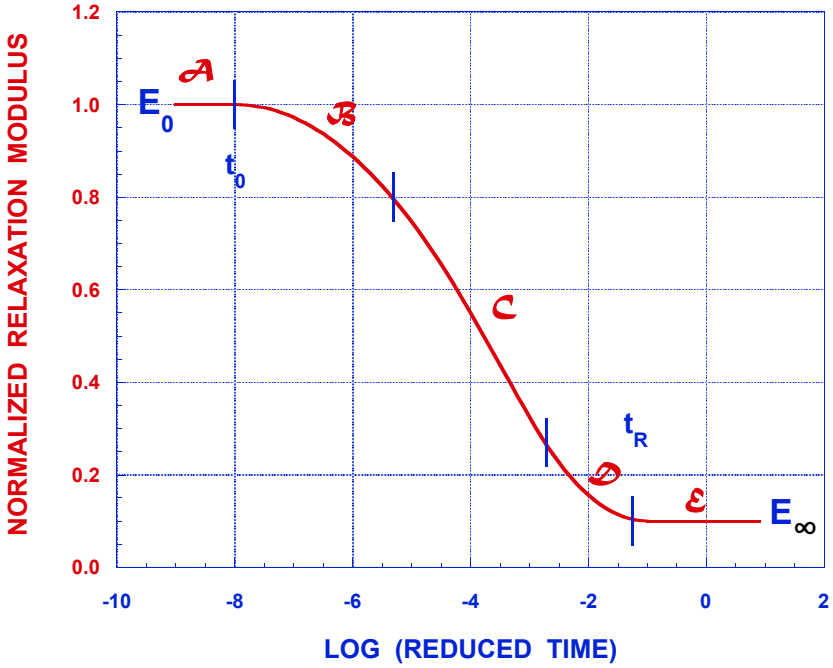

Figure 7: Regions of influence for relaxation moduli [94]

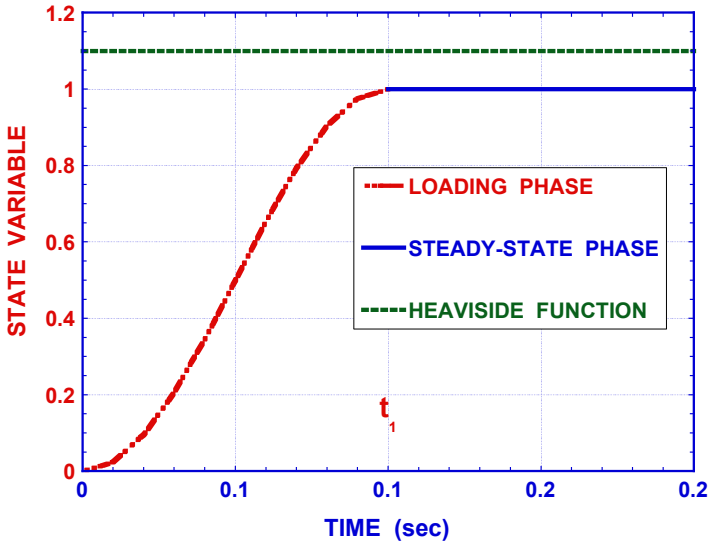

Figure 8: Starting and steady state phases

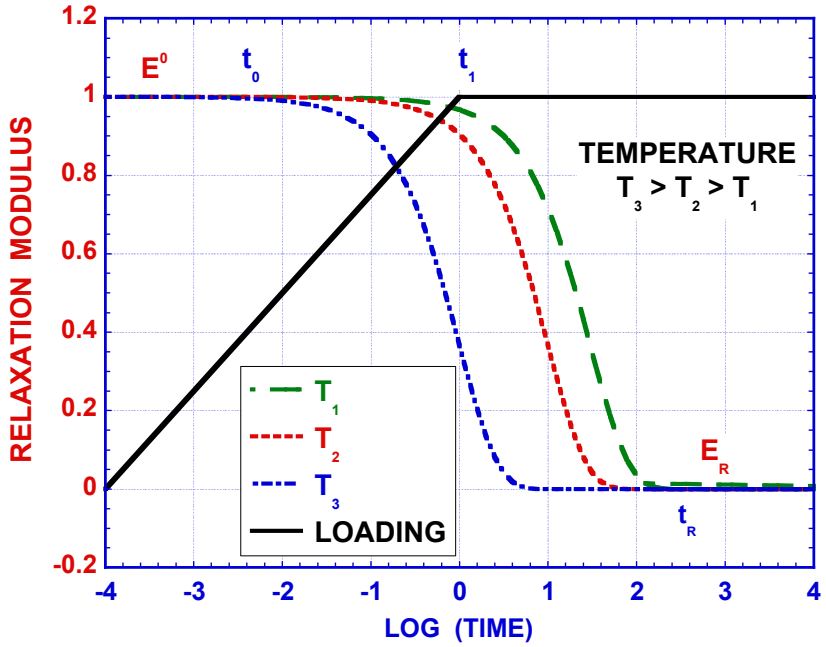

Figure 9: Loading and moduli

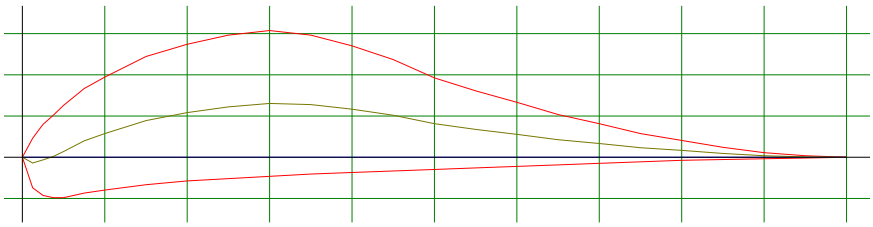

Figure 10: The Liebeck L-1003 airfoil [107]

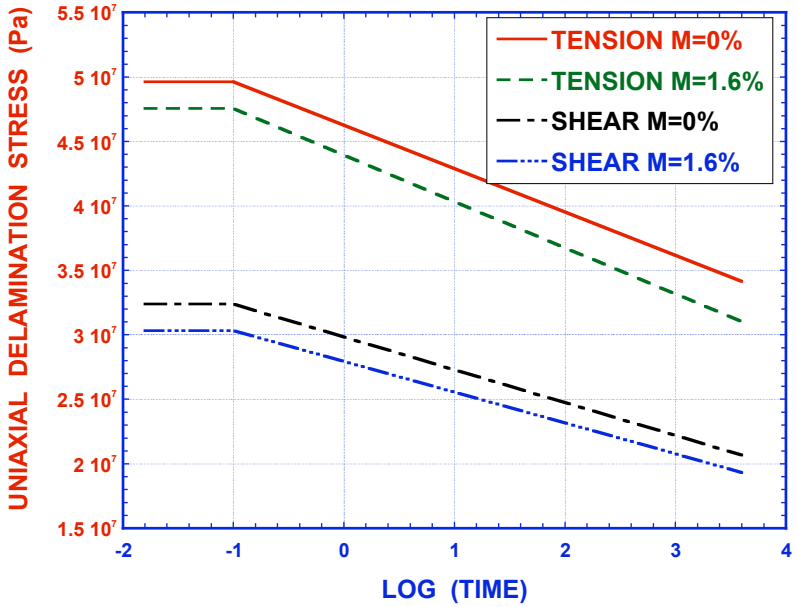

Figure 11: 1-D experimental delamination failure stresses [95]

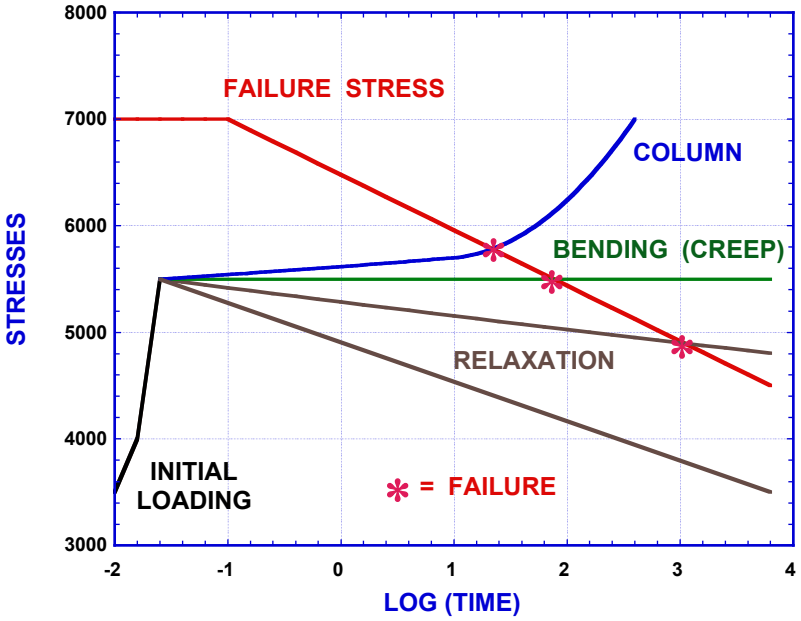

Figure 12: Impact of loading on reaching failure condition

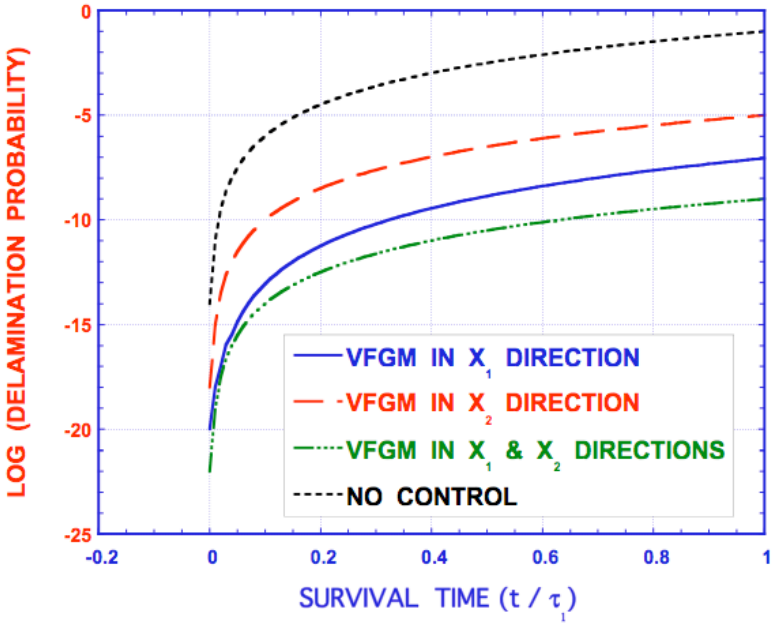

Figure 13: Influence of optimal VFGM on delamination failures

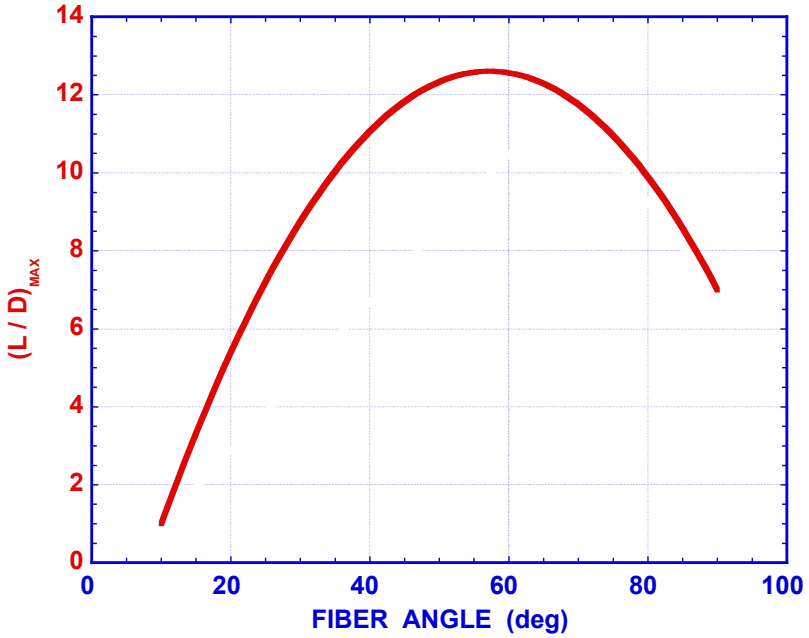

Figure 14: Ply angle dependence on L/D_{max}

employing viscoelastic functionally graded materials[3] (VFGM), which yield the best results.

For solar sails made of composite materials, such as a one consisting of multiple layers of differently oriented fibers embedded in a matrix of a distinct material, the so called ply angle of the fibers is of utmost importance as it is a fundamental contributor to the composite material properties. The second illustration, Fig. 14, demonstrates an optimum ply angle to achieve $(L/D)_{max}$ and hence an optimum solar wind thrust condition. Finally, Fig. 10 illustrates a typical optimized low drag airfoil shape derived by optimized analysis protocols.

5. Conclusions

The general system of systems analysis is simplified in an illustrative problem which demonstrates the importance of a few optimized parameters. Flight conditions can be markedly improved by adding additional variables and constraints to the simple illustrative problem. The availability of mega computers, such as as UIUC's NCSA peta scale Blue Waters [114] makes it possible to simultaneously solve in parallel large numbers of analytic and numerical relations. Hence making optimization of an entire vehicle's performance possible [112].

6. Acknowledgments

Support from the Aerospace Engineering Department in the Grainger College of Engineering and from the Computational and Data Sciences Division of the National Center for Supercomputing Applications (NCSA), both at the University of Illinois at Urbana-Champaign (UIUC), is gratefully acknowledged.

Portions of this paper were presented at the AIAA 2014 Space Conference[4] [115].

[3] essentially ordered non-homogeneous materials

[4]

7. References

[1] Balakrishnan, Arun V. (2012) *Aeroelasticity, The Continuum Theory.* Springer, New York.

[2] Bisplinghoff, Raymond L., Holt Ashley and Robert L. Halfman (1955) *Aeroelasticity.* Addison-Wesley Publishing Company, Cambridge, MA. (1980) Dover Publications, New York.

[3] Bisplinghoff, Raymond L. and Holt Ashley (1962) *Principles of Aeroelasticity.* John Wiley & Sons, New York.

[4] Destuynder, Philippe (2007) *Aéroélasticité et aéroacoustique.* Hermes Science Publications, Paris.

[5] Donaldson, Bruce K. (2006) *Introduction to Structural Dynamics.* Cambridge University Press, New York.

[6] Dowell, Earl H. (1971) "Generalized aerodynamic forces on a flexible plate undergoing transient motion in a shear flow with an application to panel flutter," *AIAA Journal* **9**:834–841.

[7] Dowell, Earl H. (1975) *Aeroelasticity of Plates and Shells.* Noordhoff International Publishing, Leyden.

[8] Dowell, Earl H. and Marat Ilganov (1988) *Studies in Nonlinear Aeroelasticity.* Springer, New York.

[9] Dowell, Earl H. and Deman Tang (2003) *Dynamics of Very High Dimensional Systems.* World Scientific, River Edge, NJ.

[10] Dowell, Earl H., Robert Clark, David Cox, Howard C. Curtis Jr., John W. Edwards, Kenneth C. Hall, David A. Peters, Robert H. Scanlan, Emil Simiu, Fernado Sisto and Thomas W. Starganac (2004) *A Modern Course in Aeroelasticity.* Kluwer Academic Publishers, Boston.

[11] Försching, Hans W. (1974) *Grundlagen der Aeroelastik.* Springer, New York.

[12] Fung, Y. C. (1955) *An Introduction to the Theory of Aeroelasticity.* John Wiley & Sons, New York.

[13] Gülçat, Ülgen (2010) *Fundamentals of Modern Unsteady Aerodynamics.* Spriger-Verlag, Berlin.

[14] Hémon, Pascal (2006) *Vibrations des structures couplées avec le vent.* École Polytechnique, Paris.

[15] Hodges, Dewey H. and G. Alvin Pierce (2002) *Introduction to structural dynamics and aeroelasticity.* Cambridge University Press, New York.

[16] Païdoussis, Michael P., (editor) (1998, 2003) *Fluid-Structure Interactions: Slender Structures and Axial Flow.* **1, 2**. Elsevier, New York.

[17] Rodden, William P. (2011) *Theoretical and Computational Aeroelasticity.* Crest Publishing, Gauteng, South Africa.

[18] Scanlan, Robert H. and Robert Rosenbaum (1951) *Introduction to the Theory of Aircraft Vibration and Flutter.* The Macmillan Co., New York.

[19] Wright, Jan R. and Jonathan E. Cooper (2007) *Introduction to Aircraft Aeroelasticity and Loads.* John Wiley, Hoboken, NJ.

[20] Hilton, Harry (1957) "Pitching instability of rigid lifting surfaces on viscoelastic supports in subsonic or supersonic potential flow," *Advances in Solid Mechanics* 1–19, Edwards Bros., Ann Arbor.

[21] Hilton, Harry H. (1960) "The divergence of supersonic, linear viscoelastic lifting surfaces, including chord-wise bending," *Journal of the Aero/Space Sciences* **27**:926–934.

[22] Chandiramani, N. K., Liviu Librescu and Jacob Aboudi (1989) "The theory of orthotropic viscoelastic shear deformable composite flat panels and their dynamic stability," *International Journal of Solids and Structures* **25**:465–482.

[23] Hilton, Harry H. and Curtis F. Vail (1993) "Bending–torsion flutter of linear viscoelastic wings including structural damping," *Proceedings AIAA/ ASME/ASCE/AHS/ASC 33rd Structures, Structural Dynamics and Materials Conference, AIAA Paper 93-1475*, **3**:1461–1481.

[24] Potapov, Vadim D. (1995) "Stability of viscoelastic plate in supersonic flow under random loading," *AIAA Journal* **33**:712–715.

[25] Kiiko, I. (1996) "Flutter of a viscoelastic plate," *Journal of Applied Mathematics and Mechanics* **60**:167–170.

[26] Drozdov, Aleksey D. (1996) "Lyapunov stability of a class of operator integro-differential equations with applications to viscoelasticity," *Mathematical Methods in the Applied Sciences* **19**:341–361.

[27] Merrett, Craig G. and Harry H. Hilton (2010) "Starting transients, lift definition and boundary condition influences on elastic and viscoelastic panel and wing flutter," *Proceedings International Conference on Mathematical Problems in Aerospace, Engineering and Sciences, Paper No. 71-4-1 PB.* Sao Jose dos Campos - SP, Brazil.

[28] Merrett, Craig G. and Harry H. Hilton (2009) "Panel flutter and aerodynamic noise attenuation through aero-servo-viscoelastic controls," *Proceedings 50th AIAA/ASME/ ASCE/AHS SDM Conference, AIAA Paper 2009-2512.* Palm Springs, CA.

[29] Hilton, Harry H., Daniel H. Lee and Craig G. Merrett (2009) "Novel protocols of matching optimized designer aero-servo-controls with engineered viscoelastic materials," *Proceedings IV ECCOMAS Thematic Conference on Smart Structures and Materials, SMART-09, Paper CD131* **CD-ROM**:1–10, Porto, Portugal.

[30] Hilton, Harry H., Daniel H. Lee and Craig G. Merrett (2009) "Wing torsional divergence avoidance through designer viscoelastic material properties and tailored aero-servo-controls," *Proceedings International Forum on Aeroelasticity and Structural Dynamics, Paper IFASD 2009-146.* Seattle, WA, 2009.

[31] Merrett, Craig G. and Harry H. Hilton (2010) "The influence of aero-viscoelastic chord-wise and unsymmetrical lifting surface bending with torsional divergence and flutter," *Proceedings Fifty-first AIAA/ASME/ASCE/ AHS/ASC Structures, Structural Dynamics and Materials (SDM) Conference, AIAA Paper 2010-2553*, Orlando, FL.

[32] Merrett, Craig G. and Harry H. Hilton (2010) "Flutter of elastic and viscoelastic panels in incompressible, subsonic and supersonic flows," *Proceedings Tenth International Conference on Recent Advances in Structural Dynamics, Paper No. 007*, Southampton, UK.

[33] Hilton, Harry H. (2010) "Aeroelasticity and aero-viscoelasticity: a critical appreciation of similarities and differences," *Proceedings Fifty-first AIAA/ASME/ASCE/AHS/ASC Structures, Structural Dynamics and Materials (SDM) Conference, AIAA Paper 2010-2702.* Reston, VA.

[34] Merrett, Craig G. and Harry H. Hilton (2019) "Generalized linear aero-servo-viscoelasticity: Theory and applications," in press it AIAA Journal.

[35] Merrett, Craig G. and Harry H. Hilton (2010) "Elastic and viscoelastic panel flutter in incompressible, subsonic and supersonic flows," *Journal of Aeroelasticity and Structural Dynamics* **2**:53–80.

[36] Merrett, Craig G. and Harry H. Hilton (2011) "Flutter initiation under steady-state and accelerated free stream velocities," *SAE International Journal of Aerospace* **4**:1449–1464. DOI: 10.4271/2011-01-2785

[37] Merrett, Craig G., Harry H. Hilton, Sahithi Kalidindi and Elliot S. Schwartz (2011) "Suppression of bending-torsion flutter in accelerated flight with aero-servo-viscoelastic controls," *Proceedings AIAA Flight Mechanics Conference, AIAA Paper 2011-6208,* Reston, VA.

[38] Merrett, Craig G. and Harry H. Hilton (2011) "Influences of starting transients, aerodynamic definitions and boundary conditions on elastic and viscoelastic wing and panel flutter," *Transdisciplinary International Journal of Mathematics, Engineering, Science and Aerospace (MESA)*, **2**:121–144.

[39] Hilton, Harry H. (2011) "Equivalences and contrasts between thermo-elasticity and thermo-viscoelasticity: a comprehensive critique," *Journal of Thermal Stresses*, **34**:488–535. DOI: 10.1080/01495739.2011.564010

[40] Merrett, Craig C. (2016) "Time to flutter theory for viscoelastic composite aircraft wings," *Composite Structures*, **154**:646–659.

[41] Merrett, Craig G. and Harry H. Hilton (2013) "Aeroelastic and aero-viscoelastic flutter issues in the age of highly flexible flight vehicles," *Transdisciplinary International Journal of Mathematics, Engineering, Science and Aerospace (MESA),* **4**:105–131.

[42] Prony, Gaspard C. F. M. R. Baron de (1795) "Essai experimental et analytique," *Journal de l'École Polytechnique de Paris*, **1**:24–76.

[43] Kottapalli, S. B. R. and G. Alvin Pierce (1979) "Drag on an oscillating airfoil in a fluctuating free stream," *ASME Journal of Fluids Engineering* **101**:391–399.

[44] Viola, Ignazio Maria (2013) "Recent advances in sailing yacht aerodynamics," *Applied Mechanics Reviews* **65**:040000-1 – 040000-12. DOI: 10.1115/1.4024947

[45] Du, Sha and Haisong Ang (2011) "Design and feasibility analyses of morphing airfoil used to control flight attitude," *Journal of Mechanical Engineering* **58**:46–55. DOI: 10.5545/sv-jme.2011.189

[46] Martins, Joaquim R. R. A. and John T. Hwang (2013) "Review and unification of methods for computing derivatives of multidisciplinary computational models," *AIAA Journal* **51**:2582–2599. DOI: 10.2514/1.J052184

[47] Weisshaar, Terrence A., Brian Prock and William A. Crossley (2002) "Morphing airfoil shape change optimization with minimum actuator energy as an objective," *AIAA Multidisciplinary Analysis and Optimization Symposium, AIAA Paper 2002-5401.*

[48] Valasek, John (Ed.) (2012) *Morphing Aerospace Vehicles and Structures.* John Wiley & Sons, Hoboken. DOI: 10.1002/9781119964032

[49] Johnston, Christopher O., William H. Mason and Cheolheui Han (2010) "Unsteady thin airfoil theory revisited for a general deforming airfoil." *Journal of Mechanical Science and Technology* **24**:2451–2460. DOI 10.1007/s12206-010-0920-4

[50] Jalili, Nader (2010) *Piezoelectric-Based Vibration Control: From Macro to Micro/Nano Scale Systems.* Springer, New York.

[51] Sabri, Farhard and S. A. Meguid (2011) "Flutter boundary prediction of an adaptive morphing wing for unmanned aerial vehicle," *International Journal of Mechanics and Materials in Design* **7**:307–312. DOI: 10.1007/s10999-011-9169-z

[52] Hilton, Harry H., D. Hank Lee and Abdul Rahman A. El Fouly (2008) "General analysis of viscoelastic designer functionally graded auxetic materials engineered/tailored for specific task performances," *Mechanics of Time-Dependent Materials* **12**:151–178. DOI: 10.1007/s11043-008-9054-9

[53] Hilton, Harry H. and Steven J. D'Urso (2013) "Designer systems of systems – A rational integrated approach of system engineering to tailored aerodynamics, aeroelasticity, stability, control, geometry, materials, structures, propulsion, performance, sizing, weight, cost," *Proceedings Fourth International conference on Inverse Problems, Design and Optimization (IPDO–2013), Paper ID 06290.* Albi, France. ISBN: 979-10-91526-01-2 Submitted to *AIAA Journal.*

[54] Anonymous (2013) "Solar wind," *Wikipedia. http://en.wikipedia.org/wiki/Solar_wind*

[55] Sutula, Ginger (2010) "Lesson: Solar wind velocity," *http://sohowww.nascom.nasa.gov/explore/lessons/swvelocity9_12.html*

[56] Villanueva, Louis (2009) "The solar wind," *http://fusedweb.pppl.gov/cpep/chart_pages/5.plasmas/SolarWind.html*

[57] Barnes, Aaron (1992) "Acceleration of the solar wind," *Reviews of Geophysics* **30**:43–55.

[58] Bruhn, Elmer F., R. John H. Bollard, Lloyd E. Hackman, George Lianis, William McCombs, A. F. Schmitt, Clarence R. Smith and Joseph A. Wol (1973) *Analysis and Design of Flight Vehicle Structures.* S. R. Jacob, Indianapolis.

[59] Liebeck, Robert H. (1973) "A class of airfoils designed for high lift in incompressible flow," *Journal of Aircraft* **10**:610–617.

[60] Liebeck, Robert H. and Alan L. Ormsbee (1970) "Optimization of airfoils for maximum lift," *Journal of Aircraft* **7**:409–415.

[61] Liebeck, Robert H. (1978) "Design of subsonic airfoils for high lift," *Journal of Aircraft* **15**:547–561.

[62] Adkins, Charles N. and Robert H. Liebeck (1983) "Design of optimum propellers," *AIAA Paper AIAA-1983-190.*

[63] Adkins, Charles N. and Robert H. Liebeck (1994) "Design of optimum propellers," *Journal of Propulsion and Power* **10**:676–682.

[64] Giguère, P. and Michael S. Selig (1998) "New airfoils for small horizontal axis wind turbines," *ASME Journal of Solar Energy Engineering* **120**:108–114.

[65] Selig, Michael S. and J. J. Guglielmo (1997) "High-lift low Reynolds number airfoil design," *Journal of Aircraft* **34**:72–79.

[66] Gopalarathnam, A., B. A. Broughton, B. D. McGranahan and Michael S. Selig (2003) "Design of low Reynolds number airfoils with trips," *Journal of Aircraft* **40**:768–775.

[67] Selig, Michael S. (2011) "PROFOIL-WWW: Airfoil design software for the web," *http://www.profoil.org*

[68] Selig, Michael S. (2013) Private communications.

[69] Eppler, Richard (1900) *Airfoil Design and Data.* Springer-Verlag, Berlin.

[70] Anonymous (2000) "Eppler airfoil design and analysis code," *http://www.airfoils.com/eppler.htm*

[71] Selig, Michael S. (2012) "The UIUC airfoil data site," *http://www.ae.illinois.edu/m-selig/ads.html*

[72] Lagrange, Joseph L. (1788) *Mécanique analytique.* Gauthier-Villars et fils, Paris.

[73] Lagrange, Joseph L. (1762) "Essai d'une nouvelle methode pour déterminer les maxima et les minima des formules integrales indéfinies," *Mélanges de philosophie et de mathématique de la Société Royale de Turin.*

[74] Anonymous (2011) http://www.ncsa.uiuc.edu/BlueWaters/

[75] Anonymous (2009) http://www.ncsa.illinois.edu/News/Stories/Kramer/

[76] Anonymous (2013) https://bluewaters.ncsa.illinois.edu

[77] Anonymous (2013) http://www.nbcnews.com/science/how-pack-big-solar-sail-tiny-cubesat-6C9765040

[78] Anonymous (2013) http://www.kickstarter.com/projects/aresinstituteinc/lunarsail-the-worlds-first-crowdsourced-solar-sail

[79] Anonymous (2013) http://www.militaryaerospace.com/articles/2013/10/nasa-solar-sail.html

[80] Woo, Byoungsam, Kevin M. Ertmer, Victoria L. Coverstone, Rodney L. Burton, Gabriel F. Benavides, David L. Carroll D. (2011) "Deployment experiment for ultralarge solar sail system (UltraSail)," *Journal of Spacecraft and Rockets* **48**:874–880.

[81] Pukniel, Andrew, Victoria L. Coverstone, Rodney L. Burton and David L. Carroll (2011) "The dynamics and control of the CubeSail mission: A solar sailing demonstration," *Advances in Space Research* **48**:1902–1911.

[82] Vulpetti Giovanni(2013) *Fast Solar Sailing – Astrodynamics of Special Sailcraft Trajectories.* Springer, New York.

[83] Vulpetti, Giovanni, Les Johnson and Gregory L. Matloff (2008) *A Novel Approach to Interplanetary Travel.* Springer, New York.

[84] Vallado, David A. and David Finkleman (2013) "A critical assessment of satellite drag and atmospheric density modeling," *Acta Astronautica* http://dx.doi.org/10.1016/j.actaastro.2013.10.005

[85] Jobson, Gary (1986) *Sailing Fundamentals.* Simon & Schuster, New York.

[86] Garrett, Ross (1996) *The Symmetry of Sailing.* Sheridan House, Dobbs Ferry. ISBN 1-57409-000-3.

[87] Anonymous (2001) *Systems Engineering Fundamentals.* Defense Acquisition University Press, Fort Belvoir, VA.

[88] Tarantola, Albert (2005) *Inverse Problem Theory and Methods for Model Parameter Estimation.* Siam, Philadelphia.

[89] Chen, Y. C. (2013) "Closed form solution for degenerate scale problem of Joukowski airfoil configuration in antiplane elasticity," *Journal of Mechanics* **29**:N21–N23. DOI: 10.1017/jmech.2013.34

[90] Timoshenko, Stephan P. (1940) *Theory of Plates and Shells.* McGraw-Hill, New York.

[91] Florjančiči, Urška and Igor Emri (2008) "Tailoring functionality and durability of polymeric products by modifying processing conditions," *Journal of Mechanical Engineering.* **54**:507–520.

[92] Janhunen, Pekka (2014) "Coulomb drag devices: electric solar wind sail propulsion and ionospheric deorbiting," *arXiv:1404.7430v1 [astro-ph.IM].*

[93] Hilton, Harry H. and Germain Sossou (2012) "Viscoelastic and structural damping analysis with designer materials," *Proceedings Fiftieth AIAA Aerospace Sciences Meeting Multidisciplinary Design Optimization (MDO), AIAA Paper 2012-1256.*

[94] Hilton, Harry H. and Sung Yi (1992) "Analytical formulation of optimum material properties for viscoelastic damping," *Journal of Smart Materials and Structures* **1**:113–122.

[95] Dillard, David A. and Hal F. Brinson (1983) "A numerical procedure for predicting and delayed failures in laminated composites," *Long Term Behavior of Composites*, T. K. O'Brien, ed., *ASTM STP 813* 23–37.

[96] Hiel, Clement, Mark Sumich and David P. Chappell (1991) "A curved beam test specimen for determining the interlaminar tensile strength of a laminated composite," *Journal of Composite Materials* **25**:854–868.

[97] Lifshitz, J. M. and A. Rotem (1970) "Time-dependent longitudinal strength of unidirectional fibrous composites," *Fibre Science and Technology* **3**:1–20.

[98] Phoenix, S. L. (1979) "Statistical aspects of failure of fibrous materials," *Composite Materials: Testing and Design, ASTM STP 674*, (S. W. Tsai, Ed.), 455–483.

[99] Phoenix, S. L. and L-J. Tierney (1982) "A statistical model for the time dependent failure of unidirectional composite materials under local elastic load-sharing among fibers," *Engineering Fracture Mechanics*, **18**:193–215.

[100] Watson, A. S. and R. L. Smith (1985) "An examination of statistical theories for fibrous materials in the light of experimental data," *Journal of Materials Science* **20**:3260–3270.

[101] Hilton, Harry H. and Sung Yi (1993) "Stochastic viscoelastic delamination onset failure analysis of composites," *Journal of Composite Materials* **27**:1097–1113.

[102] Hilton, Harry H. and S. T. Ariaratnam (1994) "Invariant anisotropic large deformation deterministic and stochastic combined load failure criteria," *International Journal of Solids and Structures* **31**:3285–3293.

[103] Green, Albert E. and Wolfgang Zerna (1954) *Theoretical Elasticity.* Oxford Press, Oxford, UK.

[104] Drozdov, Aleksey D. (1996) *Finite Elasticity and Viscoelasticity.* World Scientific, Singapore.

[105] Tadmore, Ellad B. and Ronald E. Miller (2011) *Modeling Materials: Continuum, Atomistic and Multiscale Techniques.* Cambridge University Press, New York.

[106] Lee, June G. (2012) *Computational Materials Science: An Introduction.* CRC Press, Boca Raton.

[107] Anonymous (2014) http://airfoiltools.com/airfoil/details?airfoil=l1003-il

[108] Liebeck, Robert H. (1978) "Design of Subsonic Airfoils for High Lift," *AIAA Journal of Aircraft*, **15**:547–561.

[109] Costello, George A. (1997) *Theory of Wire Rope.* Springer, New York, NY.

[110] Fuss, Melvyn A. (1987) "Production and cost functions," *The New Palgrave: A Dictionary of Economics, First Edition*, John Eatwell, Murray Milgate and Peter Newman, eds., Palgrave Macmillan, New York.

[111] Diewert, W. Erwin (1974) "Applications of duality theory," *Frontiers of Quantitative Economics.* Intrilligator, M. D. and Kendrick, K. A., eds., **2**:106–166, North-Holland, Amsterdam.

[112] Hilton, Harry H., Steven J. D'Urso and Noe Wiener (2016) "DESIGNER SYSTEMS of SYSTEMS– A RATIONAL INTEGRATED APPROACH of SYSTEM ENGINEERING to Tailored Aerodynamics, Aeroelasticity, Aero-viscoelasticity, Stability, Control, Geometry, Materials, Structures, Propulsion, Performance, Sizing, Weight, Cost," *Trans-Disciplinary Perspectives on System Complexity*, Franz-Joseph Kahlen, Shannon Flumerfelt and Anabela Alves, eds., Chapter 3:49-84, Springer, New York.

[113] Diewert, W. Erwin (2014) "Cost functions," *The New Palgrave Dictionary of Economics Online*, Steven N. Durlauf and Lawrence E. Blume. eds., Palgrave Macmillan, New York.

[114] Anonymous (2019) "Blue Waters."
http://www.ncsa.illinois.edu/enabling/bluewaters

[115] Hilton, Harry H. and Steven J. D'Urso (2014) "Astro-elastic and astro-viscoelastic system engineering: Optimum solar sail configurations based on astrodynamics, designer materials, sizing and geometries," *Proceedings AIAA SPACE 2014 Conference, AIAA Paper 2014-4203, San Diego, CA.*